

Dynamics of a Triphenylene Discotic Molecule, HAT6, in the Columnar and Isotropic Liquid Phases

Fokko M. Mulder,[†] John Stride,[‡] Stephen J. Picken,[§] Paul H. J. Kouwer,[§] Mathijs P. de Haas,[†] Laurens D. A. Siebbeles,[†] and Gordon J. Kearley^{*†}

Contribution from the Interfaculty Reactor Institute, Delft University of Technology, Mekelweg 15, 2629 JB Delft, The Netherlands, Institute Laue Langevin, BP156, Grenoble 38042 Cedex 09, France, and Polymer Materials and Engineering (PME), Department of Materials Science and Technology, Delft University of Technology, Julianalaan 136, 2628 BL Delft, The Netherlands

Received November 5, 2002; E-mail: mulder@iri.tudelft.nl

Abstract: Discotic molecules have planar, disklike polyaromatic cores that can self-assemble into “molecular wires”. Highly anisotropic charge transfer along the wires arises when there is sufficient intermolecular overlap of the π -orbitals of the molecular cores. Discotic materials can be applied in molecular electronics, field-effect transistors, and—recently with record quantum efficiencies—photovoltaics (Schmidt-Mende, L.; Fechtenkötter, A.; Müllen, K.; Moons, E.; Frien, R. H.; MacKenzie, J. D. *Science* **2001**, *293*, 1119). A combination of quasielastic neutron scattering (QENS) measurements with molecular dynamics simulations on the discotic molecule hexakis(*n*-hexyloxy)triphenylene (HAT6) shows that the dynamics of the cores and tails of discotic molecules are strongly correlated. Core and tail dynamics are not separated, the system being characterized by overall in-plane motion, on a time scale of 0.2 ps, and softer out-of-plane motions at 7 ps. Because charge transfer between the molecules is on similar time scales, these motions are relevant for the conducting properties of the materials. Both types of motion are dominated by van der Waals interactions. Small-amplitude in-plane motions in which the disks move over each other are almost entirely determined by tail/tail interactions, these also playing an important role in the out-of-plane motion. The QENS measurements reveal that these motions are little changed by passing from the columnar phase to the isotropic liquid phase, just above the clearing temperature. The model of four HAT6 molecules in a column reproduces the measured QENS spectrum of the liquid phase, suggesting that correlations persist within the liquid phase over about this number of disks.

Introduction

Discotic molecules consist of disklike polyaromatic cores to which various side groups or alkyl chains may be attached. Depending on temperature, the molecules arrange themselves in liquid crystalline phases with various degrees of mobility and disorder, e.g., nematic discotic (N_D), nematic columnar (N_{col}), and columnar hexagonal (Col_h) phases. The columnar stacks provide one-dimensional pathways for charge and energy migration with an efficiency that depends on the extent and temporal stability of the intermolecular overlap of the π systems. Efficient one-dimensional charge transfer of the liquid crystalline phase,^{2,3} together with its self-healing properties, makes these discotic materials potentially applicable in molecular electronics,

field-effect transistors, and photovoltaics. A recent example of the application of discotic molecules in photovoltaics is given by ref 1, showing record quantum efficiency in self-assembled nanostructures containing discotic molecules.

In the present study we are interested in the dynamics of the polyaromatic cores, since this is likely to play a key role in the electrical conductivities of the columns. The intermolecular charge transfer was shown to be on picosecond time scales,^{2,3} and for this reason we investigate the molecular motions on similar time scales using quasielastic neutron scattering (QENS). In systems of this size, motions occur over a wide range of time scales, and it is useful to perform a molecular dynamics (MD) simulation to identify the motions that are seen by a particular technique. In this respect QENS has the advantage that neutrons follow both the temporal and spatial characteristics of atomic motion via a well-characterized interaction with the atomic nuclei. Consequently, it is fairly straightforward to calculate the expected spectral profile by using the atomic trajectories from the MD simulation, and if this is in acceptable agreement with the observed spectra, we can not only derive which motions we are seeing, but also understand why they

[†] Interfaculty Reactor Institute, Delft University of Technology.

[‡] Institute Laue Langevin.

[§] Department of Materials Science and Technology, Delft University of Technology.

(1) Schmidt-Mende, L.; Fechtenkötter, A.; Müllen, K.; Moons, E.; Frien, R. H.; MacKenzie, J. D. *Science* **2001**, *293*, 1119.

(2) van de Craats, A. M.; de Haas, M. P.; Warman, J. M. *Synth. Met.* **1997**, *86*, 2125–2126.

(3) van de Craats, A. M.; Siebbeles, L. D. A.; Bleyl, I.; Haarer, D.; Berlin, Y. A.; Zharikov, A. A.; Warman, J. M. *J. Phys. Chem. B* **1998**, *102*, 9625–9634.

occur. Furthermore, neutrons interact strongly with protons and much less with deuterons (or carbon and oxygen), which opens the possibility to highlight or mask specific parts of the discotic molecule by isotopic labeling. QENS was successfully applied in liquid crystals,⁴ and one publication shows its application to phthalocyanine discotics.⁵

Our experiments follow hydrogen motions that occur on the picosecond time scale, but are almost totally insensitive to deuterium. By selective deuteration of the core H-atoms we can use QENS to obtain the core and chain dynamics separately, and then use the MD simulation to see how these dynamics are coupled. There are two important interactions that can be extracted from the model when it is known to reproduce the measured dynamics. First, the core/core and tail/tail van der Waals interactions are responsible for the self-assembly of the columns. Second, there is a coupling between the core motion and the motions of its tails which plays a role in the rigidity of the column, and hence alignment of the cores.

Materials and Methods

Ring-deuterated HAT6 samples were prepared by the synthesis method described by Shen et al.⁶ The degree of deuteration was 80% (Cr, 69.5 °C; D_n, 99.5 °C; I). Sample masses of about 0.5 g were used, with the powdered material being sealed in a standard thin-walled aluminum container. Temperature control was achieved using a standard cryofurnace, and counting times were about 4 h per temperature.

Quasielastic neutron spectra were obtained using the IN6 spectrometer at the Institut Laue Langevin in France. An incident wavelength of 5.9 Å was selected to give the correct compromise between energy range and energy resolution. The sample thickness was controlled to give a scattering probability of 10%. Corrections for detector efficiency, container-scattering, sample shape, etc. and conversion of the data to $S(q, \omega)$ were made using standard algorithms.

Theoretical Basis

We compare the observed incoherent scattering law with that calculated from our MD simulation. This is achieved via the Fourier transforms of the space–time correlation function, $I_s(Q, t)$:

$$S_{\text{inc}}(Q, \omega) = (1/2)\pi \int dt I_s(Q, t) \exp(-i\omega t)$$

For MD simulations it is convenient to cast the incoherent part of the intermediate scattering function, $I_s(Q, t)$, as

$$I_{\text{inc}}(Q, t) = (1/N) \sum_{\alpha} b_{\alpha, \text{inc}}^2 \langle \exp[-iQ \hat{R}_{\alpha}(0)] \exp[iQ \hat{R}_{\alpha}(t)] \rangle$$

where α is the atom label, b_{inc} is the scattering length of the nucleus, and \hat{R}_{α} is the position operator of the nucleus. The positions of the atoms as a function of time come directly from the MD simulation.

A particularly important concept in QENS is the elastic incoherent structure factor, EISF, which can be defined as the

limit of the incoherent intermediate scattering function at infinite time:

$$\text{EISF}(Q) = \lim_{t \rightarrow \infty} I_{\text{inc}}(Q, t)$$

We can now recast $I_{\text{inc}}(Q, t)$ as

$$I_{\text{inc}}(Q, t) = \text{EISF}(Q) + I'_{\text{inc}}(Q, t)$$

where $I'_{\text{inc}}(Q, t)$ decays to zero at infinite time. By taking the Fourier transform of this, we can see immediately how the data analysis is made:

$$S_{\text{inc}}(Q, \omega) = \text{EISF}(Q) \delta(\omega) + S'_{\text{inc}}(Q, \omega)$$

The EISF is the amplitude of the elastic line in the measured spectrum, and the Q -dependence of this provides information on the space confinement of the motions of the scattering atom. If the atomic motion is not confined in space (as in a liquid), there is no elastic scattering in the sense of the EISF. In the present work $S_{\text{inc}}(Q, \omega)$ and the EISF were calculated using the suite nMOLDYN.⁷

Simulation Details

A model of a single HAT6 molecule was constructed, and the structure was optimized by energy minimization with respect to the COMPASS force field.⁸ There are a number of local minima arising from the high rotational barrier of the alkoxy group, but the global minimum for an isolated molecule corresponds to neighboring alkoxy groups being alternately above and below the triphenylene ring. A copy of this molecule was then placed over the original molecule, and the structure was again optimized. This process was repeated until the S-configuration of four disks (568 atoms), illustrated in Figure 1C,D, was obtained. Again, a large number of local minima exist with energy differences rather less than $k_B T$, which are characterized by orientational phase angles between the disks of 30° and 60°. On heating and annealing, a second group of structures with an energy about 400 K higher was found in which the aromatic rings are close to superimposed when viewed along the columnar axis. An example is the L-configuration (Figure 1A,B). These structures are stable up to at least 400 K (simulation temperature), but all models were constrained by fixing two core carbon atoms on the end disks to prevent unrealistic whole-body motions and end effects of the columns during the MD simulation. The system was then thermalized at 300 K for 280 ps with a step size of 1 fs, followed by a simulation of 820 ps, again with a step size of 1 fs, which was used for the analysis. The MD simulation was then performed for the whole model, but only the dynamics of one of the center cores, with its associated chains, was analyzed for comparison with the measured spectra.

Results

The limited dynamics of a column of interacting cores (without the tails) can be modeled easily, but our main interest is how this is modified by the alkyl side chains in real discotic systems. Including the side chains introduces a large number of degrees of freedom, and we have to make a balanced choice between constraints. We prefer to limit the size of the model, and include all atoms with a high-quality force field, rather than using more “mesoscopic” methods such as united atom models. Our molecular models consist of a stack of four triphenylene

(4) Richardson, R. M. Neutron scattering from liquid crystals. In *The molecular dynamics of liquid crystals*; Luckhurst, G. R., Veracini, C. A., Eds.; NATO ASI Series, Series C, Vol. 431; Kluwer Academic: Dordrecht, The Netherlands, 1994; p 451.

(5) Belushkin, A. V.; Cook, M. J.; Frezzato, D.; Haslam, D.; Ferrarini, A.; Martin, D.; McMurdo, J.; Nordio, P. L.; Richardson, R. M.; Stafford, A. *Mol. Phys.* **1998**, *93*, 593.

(6) Shen, X.; Dong, R. Y.; Boden, N.; Bushby, R. J.; Martin, P. S.; Wood, A. *J. Chem. Phys.* **1998**, *108*, 4324.

(7) Kneller, G. R.; Keiner, V.; Kneller, M.; Schiller, M. *Comput. Phys. Commun.* **1995**, *91*, 191.

(8) Sun, H. *J. Phys. Chem.* **1998**, *102*, 7338.

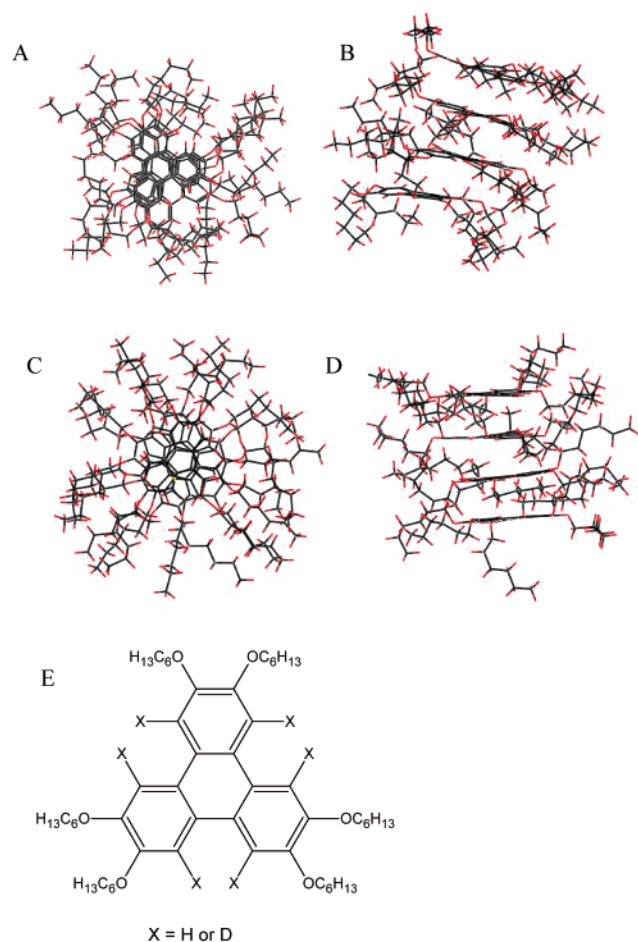


Figure 1. (A, B) Illustrations of a minimum-energy orientation with the aromatic rings nearly superimposed. (C) and (D) were minimized from a 45° phase difference between disks. (E) Schematic illustration of the HAT6 molecule.

cores each with the six side chains of $\text{O}(\text{CH}_2)_5\text{CH}_3$, for which a great many low-energy orientations were found. The two used for the present paper are illustrated in Figure 1, along with a single molecule of HAT6 for reference. By using a single short column, we ignore intercolumn interactions, and exclude long-range correlation along the column, both of which would be expected to affect the dynamics on a much longer time scale than that accessible to the current QENS experiments (possibly neutron spin-echo methods can observe these slow motions). Acoustic-like modes along the column could give rise to spectral features in the low-energy spectrum that may complicate the quasielastic spectra. However, there is little sign of structure in the measured quasielastic signal. This is due to the strong damping effect of the tails that will become clear as we describe the dynamics below.

It transpires that this model works reasonably well, but the time scale of the calculated dynamics for the model with the larger disk-disk spacing (3.7 Å, Figure 1A,B) is more rapid than that of the experimental dynamics, while the dynamics of the model with the shorter spacing (3.5 Å, Figure 1C,D) is somewhat too slow. Henceforth, these models will be referred to as “L” and “S” for long and short, respectively. In fact the L model simulation at 300 K agrees remarkably well with the measured data at 368 K, that is, just above the transition to the isotropic liquid. Here the measured quasielastic signal is not

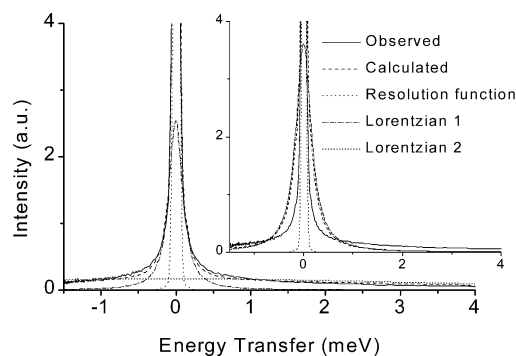


Figure 2. Comparison of observed and calculated spectra at a single Q -value, fitted with one (upper) or two (lower) Lorentzian functions and a δ function convoluted with the measured resolution function. Clearly the fit with only one Lorentzian does not describe the data properly. Spectra were fitted simultaneously over 15 Q -values.

that of a liquid, indicating that there is significant correlation between disks that closely resemble the limited size of our model.

In a complex system such as this, there will be motion over a large range of time scales, and with a single instrument only a part of this will be measured. Notwithstanding this, and the inevitable need for a molecular dynamics simulation, it is still useful to get some indication of the underlying dynamics, and how this changes with temperature and core deuteration, using a more or less conventional analysis. This is normally achieved by fitting a δ function for the elastic scattering and one or more Lorentzian functions for the quasielastic scattering, both of them convoluted with the resolution function. There is of course a limit to this (because of the number of different hydrogen atoms in the molecules), but it is instructive to see if there is a balance between the intensities and the number of core and tail hydrogen atoms.

The spectrum collected at 438 K is that of the isotropic liquid, but for the lower sample temperatures it was consistently found that at least two Lorentzian functions, in addition to the elastic peak, were required to fit the data. It transpired that one of these Lorentzians was somewhat broad, and in these cases small errors in background scattering become important. This difficulty was overcome by simultaneously fitting the spectra from different Q -values with the following constraints. Basically, at each Q -value the fitted spectrum has 2 degrees of freedom that describe how the intensity is shared between the three spectral components. In addition there are 5 global degrees of freedom expressing the widths of the two Lorentzian functions, a Debye-Waller factor, a time-of-flight flat background, and an overall scale factor. Examples of fits with one and two Lorentzians, extracted from the global fit over 15 spectra, are illustrated in Figure 2. Fits of the core-deuterated compound gave a slightly larger peak width for the broader component than the isotopically normal compound, but consistently showed a reduction in the intensity of the narrower Lorentzian component. The EISFs for the two analogues at 348 K are illustrated in Figure 3. This would suggest that the narrower peak has some contribution from core dynamics while the broader peak mainly stems from the tails, the time scales being about 0.2 and 7.7 ps, respectively. Nevertheless, the tendency for the broader peak to broaden slightly on core deuteration indicates that some core motion contributes to the broader peak. We will show later

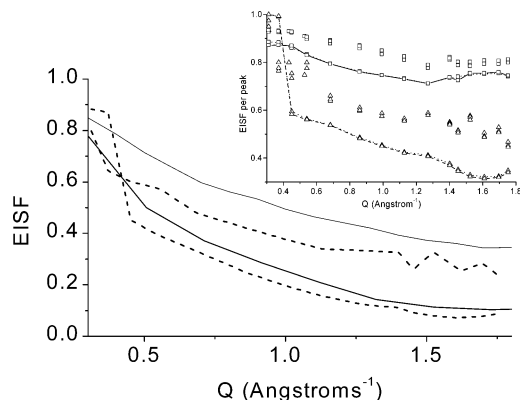


Figure 3. Observed total EISF at 348 K (upper dashed line) and 368 K (lower dashed line) compared with EISFs from simulation models S (upper solid line) and L (lower solid line) Inset: EISFs of a narrow peak (squares) and a broad peak (triangles) as a function of temperature. Unconnected symbols are for 336, 348, and 358 K (below the columnar to isotropic liquid transition), while connecting lines are used for 368 and 373 K (above the transition to the isotropic liquid). Note the change in EISF range in the inset.

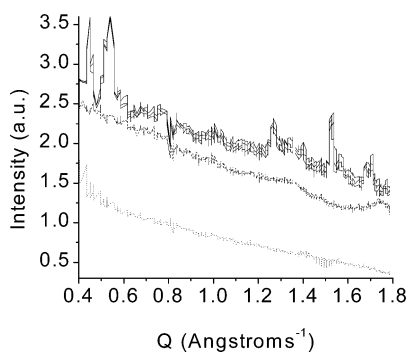


Figure 4. Elastic structure factor at 336, 348, and 358 K (overlapping solid lines at the top) showing Bragg peaks due to the liquid crystalline ordering. The dashed lines (in the middle) are for the liquid without Bragg peaks at 368 and 378 K, and the dotted line (bottom) is for 433 K.

that the core and tail motions are strongly coupled on the picosecond time scale.

Above 360 K we would expect the sample to be an isotropic liquid, but inspection of the EISFs as a function of temperature (Figure 3) reveals that this is not so. The same spectral components, with almost the same widths, are present as in the columnar phase, but there is a marked reduction in the EISF above the formal transition temperature. For an isotropic liquid we would expect a single Lorentzian spectral component with a width increasing as approximately Q^2 , and no pure elastic scattering. By inspecting $S(Q)$ (Figure 4), we can see that the Bragg peaks that characterize the columnar phase are present in the spectrum at 358 K, but are absent in the spectra at 368 and 378 K, confirming that the phase transition did indeed occur. This strongly suggests that, although macroscopically the sample is in the liquid phase, the lifetime of positional correlations between the discotic molecules is considerably longer than the longest time scale of the motions measured in this experiment. In that case the characteristic liquidlike quasielastic scattering still falls within the resolution function of the instrument and is disguised as elastic scattering. Apparently it is not unusual for complex fluids to show substantial short-range ordering in the isotropic phase.

There are two aspects to the MD simulation that arise from the limitations of the model. The starting model S has the lowest

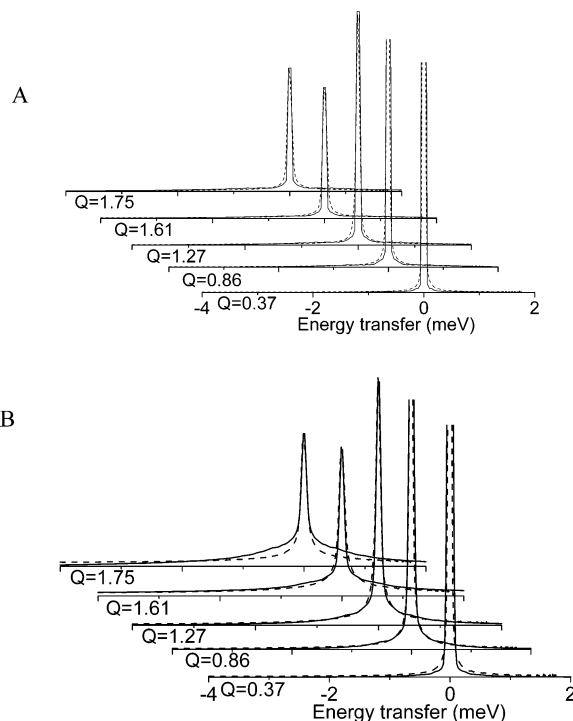


Figure 5. (A) Comparison of $S(Q,\omega)$ calculated from the simulation model S (solid line) with the measured function at 348 K (broken line). (B) Same comparison for simulation with model L and experimental data at 368 K. For each Q -value the curves have been scaled to a common maximum for ease of comparison. Q is indicated in \AA^{-1} .

energy and corresponds most closely to the crystallographic reports,⁹ the disk–disk separation being 3.5 \AA with a phase angle of around 45° between disks. Nevertheless, the calculated dynamics at 370 K corresponds best to the measured data around 340 K. This can be seen in Figure 3, where the upper solid line shows the EISF from the simulation, which is to be compared with the upper dashed line from the experiment at 348 K. This spatial limitation of the model almost certainly arises from the fixed atoms in the two end disks, a limitation that would be overcome by a larger model. We may also compare the observed and calculated quasielastic spectra as illustrated in Figure 5A. The agreement is quite satisfactory, and it is certain that a simulation temperature (or alternative force field) could be found to give still better agreement, but this is not the aim of this work. Essentially, the model compares well with the measured temporal and spatial dynamics, facilitating the identification of the origin of the measured “two-component” signal.

We now turn our attention to the solidlike quasielastic signal that we obtain from the isotropic liquid at 368 K. The S model could not produce an $S(q,\omega)$ comparable with the experiment even at 400 K, yet surprisingly, the L model with the slightly larger disk–disk separation compares very well, but in this case low simulation temperatures around 300 K are required. The simplest indication of this is in the comparison of the EISFs (Figure 3), where the lower experimental values at 368 K agree well with the simulation results. A more stringent test of the S model is a comparison of $S(Q,\omega)$ from the simulation with the measured function at 368 K, as shown in Figure 5B for different Q -values. The agreement is very satisfactory. Apparently, this particular model is representative of local structures that arise

(9) Fontes, E.; Heiney, P. A.; de Jeu, W. H. *Phys. Rev. Lett.* **1988**, *61*, 1202–1205.

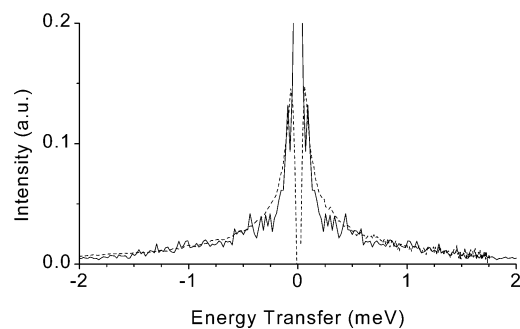


Figure 6. Comparison of calculated energy spectrum of core hydrogens at 1.61 \AA^{-1} (solid line), with the difference between measured energy spectra of HAT6 and core-deuterated HAT6 (broken line) at the same momentum transfer.

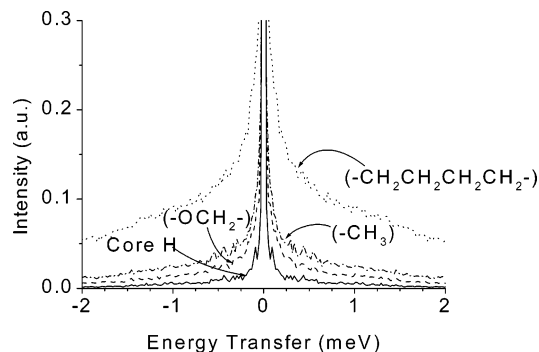


Figure 7. Energy spectra from the simulation calculated at 1.61 \AA^{-1} . These spectra were calculated separately for each of the molecular groups as labeled. The spectra have been normalized to the same maximum intensity value for ease of illustration.

due to correlated molecules in the liquid phase. There are doubtless several other models that would give a similar result, and of course similar underlying dynamics. Although it is important to start from the deepest energy minimum, there are defects, particularly in the tails, that will be quite long lived compared with the picosecond time scale of the experiment. The picosecond dynamics of these additional structures will accumulate into the measured signal, but as alluded to above, the form of the dynamics of these conformations will not differ significantly from each other and will result only in a slight change to the quasielastic peak width.

Given the general agreement, we may go further and calculate $S(Q, \omega)$ for the hydrogen atoms on the cores and compare this function with the difference between the measured spectra of the fully protonated and core-deuterated samples. This comparison is shown in Figure 6, the dip in the center of the difference spectrum arising from the normalization procedure. Nevertheless, the observed and calculated spectral profiles can be overlaid with surprising accuracy, confirming that the difference between the measured signals comes from the cores, and that our model represents all of our measured data.

Discussion

How does the primarily core motion turn over into primarily alkyl motion as we move along the chain away from the core? This could be achieved experimentally by a series of selective deuterations, but this would be expensive, so in the present work we access this from the $S(Q, \omega)$ calculated for different segments of the alkyl tails as shown in Figure 7. As expected, the motions get faster as we move out along the chain, but perhaps

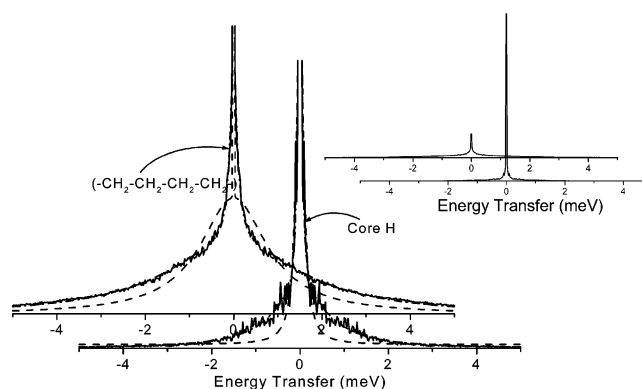


Figure 8. Calculated energy spectrum (solid line) at 0.61 \AA^{-1} for the core (lower) and central section of tails (upper) in HAT6. Fits with a Gaussian elastic peak plus one Lorentzian function (broken line) or two Lorentzian functions (dotted line) are shown. Note that the dotted line and solid line are almost coincident. The un-zoomed figures are shown in the inset to give an appreciation of the fit quality and the relative elastic peak heights.

surprisingly, central methylene groups have faster dynamics than the terminal methyl group. Further, all simulated spectra for all segments are best fitted with two Lorentzian functions, as illustrated in Figure 8. By inspection of the anisotropic mean-square amplitudes we can determine that these two separable motions for all hydrogen atoms correspond to in-plane and out-of-plane components. From the anisotropic components of the power spectrum of the different segments we see that the time scales are around 0.2 and 7 ps, respectively. So this is quite remarkable: it is not a matter of the tails and cores moving on different time scales, but a matter of basically the whole molecule moving on different time scales in different dimensions. Although the intensities and separation of these two components vary somewhat between segments, the sum of these is nonetheless the basic origin of the two-component experimental spectrum. This is true for either model, S or L. The relative intensities of the two components in the experimental EISF initially suggested that the broader component arises from the $\text{CH}_3\text{CH}_2\text{CH}_2\text{CH}_2\text{CH}_2-$ moiety, with the narrower component corresponding to core motion as seen by the core hydrogens and the $-\text{OCH}_2-$ groups. However, the simulation reveals that the effective total quasielastic line shape is the resultant of the sum of in-plane and out-of-plane motions of all hydrogens, and thus, the experimental spectra can be fitted empirically (although not perfectly) by two Lorentzian functions. Nevertheless, the core dynamics are correctly measured by the experimental difference spectrum (protonated less core-deuterated) in which the complicated tail dynamics are subtracted out. In the core dynamics the two time scales of in-plane and out-of-plane motions are present, and this too agrees with the simulation (Figure 6).

The experimental spectra in the columnar phase and the low-temperature part of the liquid phase are remarkably similar, particularly on the time scales of the dynamics. The principal difference is that the overall EISF decreases as the columnar phase transforms into the liquid, presumably resulting from the loss of ordered column/column interactions, alongside a loss of coherence length within a column. In the model S, this difference would seem to arise from an increase in the spacing between the disks. For real applications it is the columnar phase that is of interest, and we can now understand what sort of model

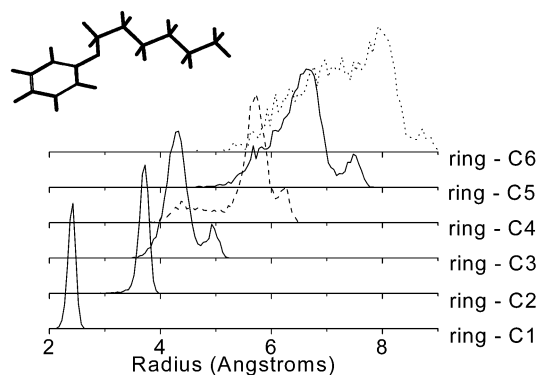


Figure 9. Radial distribution functions, $g(r)$, between a core carbon atom and each of the carbon atoms on the attached tail. For clarity, the functions have been normalized on their maxima, and for C4 and C6 a different line type is used. The inset shows a tail conformation relative to the core aromatic ring consistent with the maxima in the six functions.

we require to address that question, and what experimental data are required to validate the model.

The MD simulations reveal a number of interesting aspects of the core and chain dynamics. At the simulation temperature there is only restricted rotation of the cores, there being a tendency for the cores to slide over each other to positions where the aromatic rings remain approximately superimposed when viewed along the column axis. This is not dissimilar to the proposals of Leisen et al.¹⁰ Rotation of the cores relative to each other is slow, and while partial rotation occurred during the simulation period, no full rotation was observed. It will be possible to describe the rotation process as a diffusion process that occurs on time scales much longer than that accessed by our simulation. Using nuclear magnetic resonance relaxation measurements, Shen et al.⁶ were able to determine that full rotations occur on a 10 ns time scale, which is indeed much longer than our simulated time span.

The preferred orientations of the alkyl tails (and excursions from these) can be deduced from the calculated (from the simulation) radial distribution function, $g(r)$, between the terminal carbon atom and the core carbon atom to which the tail is attached. The strongest peaks in these functions (Figure 9) are at 2.4, 3.7, 4.2, 5.7, 6.6, and 8.0 for the ring carbon to C1–C6, respectively, corresponding to the distances in a low-energy configuration of the tail as shown in the inset. The O–C1–C2–C3 conformation is approximately *cis*, while all other dihedral orientations of the tail are close to *trans*. Weaker peaks on the right of the main peaks in $g(r)$ arise from the more extended *all-trans* conformation, while the wings on the left side correspond to more compact tail conformations. However, the dominance of a single peak in the $g(r)$ functions reveals a marked tendency for the tails to remain close to the molecular plane of the aromatic core, which was also noted in the animation. This is particularly marked for carbon atoms C1–C4. The radial distribution function between terminal carbon atoms on neighboring tails linked to different cores (not shown) also shows that the tails tend to remain in-plane ($g(z)$, the $g(r)$ parallel to the column axis, peaks at about the interdisk distance), but also shows occasional excursions even over next-neighbor rings. Recent work with discotics having alternately long and

Table 1. Force Constants Resulting from MD Simulations

	force constant of the core (kcal mol ⁻¹ Å ⁻²)	force constant of the tails (kcal mol ⁻¹ Å ⁻²)
Δ van der Waals in plane	3.3	60.1
Δ Coulomb in plane	5.7	4.4
Δ van der Waals out of plane	165.2	455.3
Δ Coulomb out of plane	1.1	3.1

short tails on the same disk¹¹ proposes a mesoscopic picture in which the long and short tails stick out from each core, with a coglike meshing (interdigitation) between columns. Our work suggests that a temporal coincidence of identically extended tails on neighboring columns will be unlikely (see $g(r)$ for the terminal carbon atom, C6, in Figure 9).

The picture that emerges from the experimental data and the simulation is of strongly correlated core and tail motions, this persisting to a limited degree even at the terminal methyl group. Thus, as already stated above, it is in this situation more appropriate to distinguish in-plane and out-of-plane motions that underlie the dynamics, rather than core dynamics and tail dynamics.

We will now try to understand which interactions are responsible for this behavior. Using the same force field as for the simulation, we calculate an energy gain of 40 K for each HAT6 molecule that is added to a column, this gain being almost entirely due to van der Waals interactions. For the dynamics, however, we are more interested in the net force constants for in-plane and out-of-plane motion, and what the relative contributions of core and tail interactions are in these. We determined two force constants numerically as the second derivative of the energy by making two successive displacements of a whole molecule in the plane, and out of the plane. By making energy calculations based separately on tails and cores, these contributions can be separated. The results are collected in Table 1, from which it is clear that—as expected—van der Waals interactions dominate, and that the in-plane force constants are considerably higher than their out-of-plane counterparts. Interestingly, the in-plane force constant for the tails is much higher than that for the cores, although clearly lower values would be obtained if the tails were allowed to relax after each displacement. Nevertheless, it is clear that tail/tail van der Waals interactions determine the rigidity of the columns. This may be understood intuitively on the basis of the thickness of the core (flat without groups out-of-plane on it) that is smaller than the thickness of the three-dimensional tail. It would be interesting to explore the dynamics of a system in which each core has a variety of tail lengths attached or special “bulky” groups. In this respect the main effect of short and long tails¹¹ would be to reduce intracolumn slipping between neighboring disks, rather than to link the rotations of neighboring columns.

Recently,¹² it has been shown that hole mobility in binary mixtures of triphenylene derivatives are an order of magnitude higher than for the separate components, this being attributed to a more stable columnar structure. This may illustrate that the tail/tail interaction plays an important role in column rigidity. van der Waals tail/tail interaction also plays an important role in the out-of-plane motion. Calculated hole mobilities in discotic

(10) Leisen, J.; Werth, M.; Boeffel, C.; Spiess, H. W. *J. Chem. Phys.* **1997**, *97*, 3749.

(11) Allen, M. T.; Diele, S.; Harris, K. D. M.; Hegmann, T.; Kariuki, B. M.; Lose, D.; Preece, J. A.; Tschierske, C. *J. Mater. Chem.* **2001**, *11*, 302.

(12) Wegewijs, B. R.; Siebbeles, L. D. A. *Phys. Rev. B* **2002**, *65*, 245112.

materials are considerably higher than those measured,¹² this being attributed to disorder. The system moves between a large number of closely spaced potential-energy minima, the resultant motions being rather anharmonic. In our simulation the amplitudes of these in-plane and out-of-plane motions are 0.3 and 1.2 Å, respectively, for the solid phase (model S), showing how large the disorder can be. It would be interesting to extract low-energy configurations from either an MD simulation or a Monte Carlo method, and use these for the calculation of hole mobility.

As far as we know discotic liquid crystalline materials have been studied only once before using neutrons: Belushkin et al. studied a phthalocyanine derivative.⁵ However, much work on the structure and dynamics of discotics has been performed using nuclear magnetic resonance (see, e.g., refs 6, 13, and 14 and references therein). It is interesting to compare the work presented here with the results obtained by nuclear magnetic resonance (NMR). It should be realized that neutron scattering and NMR are complementary techniques with respect to the time scales that they are sensitive to: neutron techniques can be sensitive to femtosecond to 10^2 ns time scales, whereas NMR techniques can be sensitive to ~ 0.2 ns to second time scales. Because intermolecular charge-transfer processes in these materials are extremely rapid, i.e., on picosecond time scales, the molecular dynamics as observed with neutrons can be interfering directly with the charge transfer. This means that this fast molecular dynamics may determine the instantaneous intermolecular electron wave overlap, and short-range intermolecular conductivities. The slower dynamics observable by NMR can interfere with the charge transfer on longer length scales; i.e., it could be showing the temporal defects in the columnar structure that limit long-range conductivity. Shen et al. discuss the presence of rotational diffusions D_{\perp} and D_{\parallel} (respectively, perpendicular and parallel to the column axis) on time scales of 10^{-8} s for HAT6 in the columnar liquid crystalline phase using NMR results.⁶ They conclude that with NMR only motions are observed on slow time scales compared to the intermolecular charge transfer and that to the migrating charges the lattice therefore appears static. We clearly have to refine this statement, stating that with neutrons we observe molecular motions in and out of the molecular plane on 0.2 and 7 ps time scales, respectively. These motions will change the instantaneous overlap of electronic wave functions, and will therefore modify the conductivity. Full rotations of the molecules will indeed be on the slower time scales as observed by NMR, because the

MD simulations confirm that such rotations are slower than on nanosecond scales (many fast diffusive partial rotations are expected to add up to full rotations). NMR observes the environments time averaged with respect to the picosecond mobility, where it is capable of sampling slower time scale dynamics.

Conclusions

The dynamics of the triphenylene derivative HAT6 has been studied using QENS and MD simulations. To the best of our knowledge, this is the first study of this kind on an important model system for these technologically relevant discotics. The results show that the dynamics of the inner core and the alkyl tails are strongly correlated. Two time scales are found to dominate the dynamics: in-plane and out-of-plane motions, the first of which has the smallest time scale. It appears that at temperatures just above the liquid crystalline to isotropic liquid phase transition there still are relatively long lived correlations of the molecular orientations, but with a strongly reduced correlation length.

The main interest in these compounds is the conductivity along the columns. Quantum chemistry calculations on minimum-energy conformations provide important information in this respect, but at present vast computing resources would be needed to use these for dynamics on the relevant time scales. By using a force field that is parametrized via quantum chemistry calculations, it is possible to run simulations on modest models using more ordinary workstations. We have shown the complementarity with experiment both for validating the simulation and for understanding the origin of the measured signals.

The tails play a central role, and because these are correlated with the cores, it is quite difficult to separate the core and tail interactions from the experimental data alone. It would be interesting to verify the core/core interactions using ab initio methods, since the empirical method used in this work is rather approximate for overlapping π -systems. Knowing the representative displacements from the present study, it should now be possible to quantify the effect of the core dynamics on the conductivity along the columns and then to determine what role the dynamics plays in the correlation length.

Acknowledgment. We are grateful to R. Richardson for useful discussions and to O. R. Lozman for providing samples. This work received financial support from the Netherlands Organization for Scientific Research (NWO) via Grant No. CW 700.51.022.

JA029227F

(13) Herwig, P.; Kayser, C. W.; Mullen, K.; Spiess, H. W. *Adv. Mater.* **1996**, *8*, 510.

(14) Brown, S. P.; Spiess, H. W. *Chem. Rev.* **2001**, *101*, 4125–4155.